amcs

ANALYTICAL PERFORMANCE ANALYSIS OF THE M2M WIRELESS LINK WITH AN ANTENNA SELECTION SYSTEM OVER INTERFERENCE LIMITED DISSIMILAR COMPOSITE FADING ENVIRONMENTS

DANIJEL ĐOŠIĆ [a], DEJAN MILIĆ [b], NATAŠA KONTREC [a,*], ČASLAV STEFANOVIĆ [c],
SRĐAN MILOSAVLJEVIĆ [d], DUŠAN M. STEFANOVIĆ [e]

[a] Faculty of Sciences and Mathematics
University of Priština in Kosovska Mitrovica
Lole Ribara 29, 38220 Kosovska Mitrovica, Serbia
e-mail: natasa.kontrec@pr.ac.rs

[b] Faculty of Electronic Engineering
University of Niš
A. Medvedeva 14, 18000 Niš, Serbia

[c] Department of Signal Theory and Communications
Charles III University of Madrid
28911 Leganes, Spain

[d] Faculty of Economics
University of Priština in Kosovska Mitrovica
Kolašinska 156, 38220 Kosovska Mitrovica, Serbia

[e] College of Applied Technical Sciences in Niš
A. Medvedeva 20, 18000 Niš, Serbia

This paper considers direct mobile-to-mobile (M2M) communications with a dual antenna selection (AS) system at a destination mobile node (DMN) in interference limited, dissimilar composite fading environments. In particular, we model dissimilar interference limited signals at the inputs of the dual branch AS system as (i) the ratio of two Nakagami-m (N) random variables (RVs) at the first branch and (ii) the ratio of two Rice RVs at the second branch, in order to account for non line-of-sight (NLOS) and line-of-sight (LOS) communications, respectively. Moreover, we assume variable powers of the desired as well as interference signals at the output of the DMN in order to account for the impact of shadowing. For the proposed model, we derive probability density functions, cumulative distribution functions, outage probabilities and average level crossing rates. The derived statistical results are evaluated for all the statistical measures considered and are graphically presented in order to provide insight into the impact of composite fading severities and LOS factors for the desired signal, as well as for the interference, on the system performances.

Keywords: mobile-to-mobile communication, vehicle-to-vehicle communication, Nakagami-m fading, Rice fading, probability density functions, cumulative density functions.

1. Introduction

Wireless mobile systems play an important role in everyday communications. Among the connected devices there are not only mobile phones but also sensors,

vehicles, trains, drones, machines, etc. (Sun *et al.*, 2021). Near-future, next-generation of communications (5G and beyond) requires new technologies in order to provide reliable and safe communications at any data speed, for any type of wireless receivers, and for any particular scenarios (Agiwal *et al.*, 2016).

---

*Corresponding author

5G systems are often under the influence of very dynamical time varying channels due to the mobility and density of movable nodes (Wu and Fan, 2016), especially in the case of mobile-to-mobile (M2M) and vehicle-to-vehicle (V2V) communications (Mumtaz *et al.*, 2014; Bithas *et al.*, 2017). Wireless propagation from the source node to the destination node is carried out through various paths that have different delays, signal attenuations, and phase shifts, causing the so-called fading phenomena. In general, the fading phenomena consist of multipath fading (due to transmission over multiple geometrical paths) and shadowing (due to various obstacles between the source and the destination). Moreover, multipath fading is characterized by signal envelope fluctuations while shadowing is characterized by variable mean power.

The wireless radio propagation is significantly influenced by the environments. In M2M and V2V communications, objects with strong influence are buildings, vehicles, hills, trees, etc., depending on the actual size, number and density of those objects. Other non-negligible phenomena that exist in mobile communications are co-channel interference (present mainly due to reuse of carrier frequency in cellular communications), and noise. Interference-limited fading (where the impact of interference is much stronger than noise, so that noise can be neglected) can be efficiently modeled as a ratio of two random variables (Silva *et al.*, 2019). Moreover, the antennas on the mobile connected nodes are positioned relatively at the same horizontal plane, which may cause extra impairments during communications.

In particular, selection combining techniques over different fading channels is explored by Milic *et al.* (2016) and Khedhiri *et al.* (2014), while macro-diversity systems by exploiting selection antennas at the macrolevel are investigated by Sekulović *et al.* (2018) and Djosic *et al.* (2019). The distributed antenna systems with selection over correlated fading channels are addressed by Agiwal *et al.* (2016). Furthermore, performance evaluation of V2V, cooperative V2V, M2M, macro-diversity V2I (vehicle-to-infrastructure) systems is considered by Bithas *et al.* (2017), Stefanovic *et al.* (2018a), Bithas *et al.* (2018b) and Stefanovic *et al.* (2018b), respectively. Transmit selection antenna systems for NOMA based vehicular systems and UAV (unmanned-aerial-vehicle) to ground communications are taken into consideration by Jaiswal and Purohit (2021), Bithas *et al.* (2020), Stefanovic *et al.* (2021) or Dixit *et al.* (2021).

A Nakagami-m (N) random variable (RV) can be used to account for the impact of multipath fading in non line-of-sight (NLOS) environments, while a Rice random variable (RV) can be used to account for the impact of multipath fading in LOS environments (Panic *et al.*, 2013). A Gamma (G) RV is usually

applied to address shadowing due to its mathematical tractability and appropriate fittings with experiments (Kostić, 2005). Earlier research (Shankar, 2004) provides a generalized composite fading model (where the composite fading environment is characterized by the simultaneous presence of multipath fading and shadowing) composed by averaging the product of conditioned N and G RVs over the mean power of a G RV. Relaying M2M scenarios in the presence of interference are further investigated by Hajri *et al.* (2020), Bithas *et al.* (2018a), Djošić *et al.* (2017) or Milosevic *et al.* (2018a) in terms of first- and second-order statistics. It is important to note that the second order statistics (level crossing rate (LCR) and average fade duration (AFD)) can provide new insights about M2M propagation channels, since LCR and AFD are influenced by a Doppler spread which, in turn, plays a significant role in high mobility and high speed propagation environments.

The second-order statistics of multiple-input-multiple-output (MIMO) systems are considered by Abdi *et al.* (2003) and Ivanis *et al.* (2007). Moreover, important second order statistics for V2X communications scenarios are investigated by Bithas *et al.* (2017), Stefanovic *et al.* (2018a; 2018b) and Huang *et al.* (2020). Moreover, LCR and AFD for 5G millimeter wave communications are further explored by Marins *et al.* (2021).

In M2M communications over highly dynamical, time varying fading channels, the line of sight (LOS) is hard to establish and attain during the whole transmission time. Motivated by the fact that M2M communication in an LOS/NLOS interference limited fading environment over dissimilar fading channels will lead to relatively less complex mathematical formulas compared with the scenarios over general or similar fading channels (Milosevic *et al.*, 2018a; 2018b; Djošić *et al.*, 2017), in this paper we consider first- and second-order statistics of the ratio of two N RVs as well as two R RVs with application to a realistic scenario for an M2M communication system. In order to account for interference limited fading environments over an LOS as well as non LOS communications, we propose a dual branch antenna selection (AS) system at the destination mobile node (DMN) over dissimilar fading modeled as the ratio of two N RVs at the first branch and the ratio of two R RVs at the second branch. The mitigation of the shadowing influence is addressed at the output of the M2M with two AS systems by averaging mean powers of G RV for all statistical measures considered. In this paper we obtain novel closed-form exact expressions for the probability density function (PDF), the cumulative distribution function (CDF) and the average LCR of the ratio of two N RVs and two R RVs at the output of the dual-input AS system. The contribution of this paper are novel analytical expressions with application to M2M AS

based communication systems.

To the best of our knowledge there are no previous results on the first-and second-order statistics of M2M with two AS diversities over the interference limited, dissimilar composite fading channel, modeled as the ratio of two N and two R RVs and averaged by G RVs at the output of the proposed system.

The remainder of the paper is organized as follows: First the system model is explained briefly in Section 2, with most important devices and effects highlighted. An antenna selector represents a starting point for further analysis, together with the appropriate signals at its inputs and its output. Section 3 outlines the results obtained for the NLOS signal path, which is assumed to be the signal present on one of the two antennas, which is not directive. Section 4 determines the relevant results for the LOS environment, or the signal present at the other antenna that directly points backwards from the rear of the vehicle. In Section 5, the combined performance of the complete antenna system is analyzed with the assumption that the useful signals, as well as interferences are subject to mutually uncorrelated shadowing effects. Numerical results are shown and discussed in Section 6, which is followed by conclusions in Section 7.

2. System model

M2M communication between a mobile source node (MSN) and a mobile destination node (MDN) with a dual-branch antenna selection (AS) reception system at the MSN exposed to multipath fading and shadowing, resulting in LOS and NLOS signals at the MDN is presented in a simplified system model of Fig. 1. Moreover, it is assumed that the LOS as well as NLOS channels are also subjected to the influence of the interferences.

The antenna selection (AS) system of the mobile destination node (MDN) receiver, with two antennas (inputs) has been proposed in order to improve performances of the proposed complex composite fading interference limited environment; its block scheme is shown in Fig. 2.

At the first input, the presence of the desired signal and interference are denoted as ζ_1 and η_1, respectively, while at the second, the input desired signal and interference are denoted as ζ_2 and η_2, respectively. Moreover, the signal-to-interference ratios (SIRs) are denoted as ϑ_1 and ϑ_2, respectively.

It is assumed that the useful signal, represented by a random variable ζ_1, is coming from one of the antennas that is NLOS, or not highly directive, as in the cases of highly directive antennas, one can easily lose the signal when the vehicle turns at bends. Therefore, the interference at this antenna, represented by a random variable η_1, is assumed to be significant, since it can pick
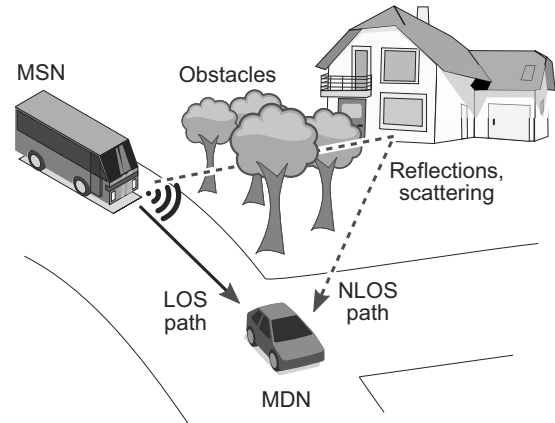

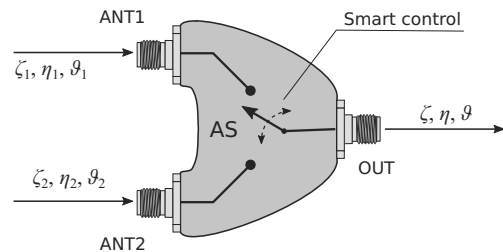Fig. 1. Simplified system model.

Fig. 2. Block diagram of the AS combiner with two inputs.

up the signals from a wider distribution of angles.

The other antenna is responsible for LOS signals, and it should be highly directive, since the goal is to exploit the favorable conditions when there is a clear line of sight between the receiver and the transmitter that is located directly backwards from the receiver. The random variable that represents the useful signal on this input is denoted by ζ_2, while the interfering signals that may exist in the same frequency range are represented by the random variable η_2.

The random variables at the AS output are the useful signal ζ, the interference η, and the SIR ϑ. The receiver yields that ϑ is equal to ϑ_1 when $\vartheta_1 > \vartheta_2$, while the signal ϑ is equal to ϑ_2 when $\vartheta_2 > \vartheta_1$. It should be noted that the selector is completely symmetrical, and therefore it does not have preferences for LOS or NLOS antenna ports. Nevertheless, we assume that the NLOS antenna is connected on Port 1 and the LOS antenna on Port 2. In general, the overall performance should be independent of the port choice.

In principle, there are different ways in which the antenna signals can be combined. One approach would be equal gain combining (EGC), where the signals are added together after aligning their phases. The advantage of such combining would be in using the available information from both antennas at the same time, but there is a requirement of co-phasing the signals that adds significant

complexity to the combiner, which in some cases can cancel the good sides of this approach. Another possibility is maximal ratio combining (MRC) that combines signals from both the antennas, but with variable gain so that optimal performance can be achieved. Once again, the added complexity of co-phasing and controlling the individual gains can overturn the usefulness of the approach. Selection combining (SC), as used in the AS, is the simplest approach that usually shows lower performance, but is robust and simple to implement, and does not require co-phasing RF signals. Therefore, due to its robustness, low complexity and resulting reliability, it may be a good candidate for automotive use.

3. Outage statistics over the NLOS signal path in the presence of interference

Here we provide statistical analysis of the proposed model in terms of (i) the probability density function (PDF), (ii) the cumulative density function (CDF), and (iii) the level crossing rate (LCR) of two Nakagami-m (N) RVs in order to address M2M communication over the NLOS signal path in the presence of interference.

Here ζ_1 has an N PDF (Panic *et al.*, 2013):

$$p_{\zeta_1}(\zeta_1) = 2\frac{\zeta_1^{2m_1-1}}{\Gamma(m_1)}\left(\frac{m_1}{\Omega_1}\right)^{m_1}\exp\left(-\frac{m_1}{\Omega_1}\zeta_1^2\right),$$
$$\zeta_1 > 0. \quad (1)$$

The parameter $m_1 > 1/2$ determines the fading severity of the environment, and smaller values of m_1 correspond to more severe fading in the channel. Ω_1 is the mean square of the signal. The interference signal η_1 also has an N PDF (Panic *et al.*, 2013):

$$p_{\eta_1}(\eta_1) = 2\frac{\eta_1^{2m_2-1}}{\Gamma(m_2)}\left(\frac{m_2}{s_1}\right)^{m_2}\exp\left(-\frac{m_2}{s_1}\eta_1^2\right),$$
$$\eta_1 > 0. \quad (2)$$

The mean square of the interference is s_1, while fading severity is determined by parameter $m_2 > 1/2$.

In an interference limited NLOS environment, ϑ_1 can be equal to the ratio of the two N random variables (Milosevic *et al.*, 2018b; 2017; Talha and Patzold, 2011; Pavlović *et al.*, 2013; Stefanovic *et al.*, 2019; Milenkovic *et al.*, 2017):

$$\vartheta_1 = \frac{\zeta_1}{\eta_1}. \quad (3)$$

The PDF of ϑ_1 is then (Panic *et al.*, 2013)

$$p_{\vartheta_1}(\vartheta_1) = \int_0^{+\infty} \eta_1 p_{\zeta_1}(\vartheta_1\eta_1)p_{\eta_1}(\eta_1)\,\mathrm{d}\eta_1$$
$$= 2\frac{\Gamma(m_1+m_2)}{\Gamma(m_1)\Gamma(m_2)}\frac{(m_1s_1)^{m_1}(m_2\Omega_1)^{m_2}\vartheta_1^{2m_1-1}}{(m_1s_1\vartheta_1^2+m_2\Omega_1)^{m_1+m_2}}. \quad (4)$$

Furthermore, the CDF of ϑ_1 is (Panic *et al.*, 2013):

$$F_{\vartheta_1}(\vartheta_1) = \int_0^{\vartheta_1} p_{\vartheta_1}(t)\,\mathrm{d}t$$
$$= 2\frac{\Gamma(m_1+m_2)}{\Gamma(m_1)\Gamma(m_2)}(m_1s_1)^{m_1}(m_2\Omega_1)^{m_2} \quad (5)$$
$$\times \int_0^{\vartheta_1} \frac{t^{2m_1-1}\,\mathrm{d}t}{(m_1s_1t^2+m_2\Omega_1)^{m_1+m_2}}.$$

The previous integral can be evaluated using the definition of the incomplete Beta function (Gradshteyn and Ryzhik, 2000):

$$\int_0^{\lambda} \frac{x^m\,\mathrm{d}x}{(a+bx^n)^p} \quad (6)$$
$$= \frac{a^{-p}}{n}\left(\frac{a}{b}\right)^{(m+1)/n}\mathrm{B}\left(\vartheta;\ \frac{m+1}{n},p-\frac{m+1}{n}\right),$$

$$\vartheta = \frac{b\lambda^n}{a+b\lambda^n}, \quad a>0, \quad b>0,$$
$$n>0, \quad 0<\frac{m+1}{n}<p.$$

With the substitution above, we get

$$F_{\vartheta_1}(x) = \frac{\Gamma(m_1+m_2)}{\Gamma(m_1)\Gamma(m_2)}$$
$$\times \mathrm{B}\left(\frac{m_1s_1x^2}{m_2\Omega_1+m_1s_1x^2};\ m_1,m_2\right). \quad (7)$$

As already stated in the introduction, second-order statistics represent important performance metrics related to mobility (Bithas *et al.*, 2017; Khedhiri *et al.*, 2014; Stefanovic *et al.*, 2018a; 2018b; Hajri *et al.*, 2020; Milosevic *et al.*, 2018a). We find the most important of them to address the level crossing rate (LCR), which can be calculated as the average value of the first derivative of the random process (Panic *et al.*, 2013). We consider the random variable ϑ_1 as a ratio of independent random variables ζ_1 and η_1,

$$\vartheta_1 = \frac{\zeta_1}{\eta_1},$$
$$\dot{\vartheta}_1 = \frac{\dot{\zeta}_1}{\eta_1} - \frac{\zeta_1}{\eta_1^2}\dot{\eta}_1,$$
$$\overline{\dot{\vartheta}_1} = \frac{\overline{\dot{\zeta}_1}}{\eta_1} - \frac{\zeta_1\overline{\dot{\eta}_1}}{\eta_1^2} = 0, \quad (8)$$

where $\dot{\zeta}_1$, $\dot{\eta}_1$ and $\dot{\vartheta}_1$ are the first derivatives of ζ_1, η_1, and ϑ_1, respectively, and where the mean values of ζ_1 and η_1

are $\bar{\zeta}_1 = \bar{\eta}_1 = 0$. Obviously, $\dot{\vartheta}_1$ has a Gaussian PDF. Moreover, the first derivative of an N random variable is a Gaussian random variable (Jakes and Cox, 1994). Also, any linear transformation of a Gaussian random variable results in a Gaussian random variable (Jakes and Cox, 1994). The variance of $\dot{\vartheta}_1$ is

$$\sigma_{\dot{\vartheta}_1}^2 = \frac{1}{\eta_1^2}\sigma_{\dot{\zeta}_1}^2 + \frac{\zeta_1^2}{\eta_1^4}\sigma_{\dot{\eta}_1}^2, \qquad (9)$$

where the variances of $\dot{\zeta}_1$ and $\dot{\eta}_1$ are

$$\sigma_{\dot{\zeta}_1}^2 = \pi^2 f_m^2 \frac{\Omega_1}{m_1}, \quad \sigma_{\dot{\eta}_1}^2 = \pi^2 f_m^2 \frac{s_1}{m_2}. \qquad (10)$$

respectively.

In the previous equation, f_m represents the maximum frequency deviation due to the Doppler shift. The frequency shift results from relative movements of the transmitter, the receiver, as well as the reflecting objects that are involved in signal propagation between the two. When the transmitter and the receiver move towards each other, the Doppler shift is positive, while it is negative in the opposite case. However, the overall situation is much more complex, as there are multiple reflectors (for example, other vehicles) that may be moving with various speeds and directions, or some static ones that vehicles move relative to (e.g., traffic signs, posts, infrastructure, etc.). As the number of waves that converge at each antenna is large, the resulting Doppler shift can be considered zero-mean normally distributed, with dispersion modeled as in the previous equation. Therefore, f_m represents the largest relative velocity between relevant objects that affect propagation.

The instantaneous frequency is by definition the time derivative of a signal, and we are considering the base band equivalents of RF signals where the carrier frequency is translated to zero. Therefore, the total frequency shift is represented by a zero-mean Gaussian random variable that is statistically independent of the signal itself. Substituting (10) into (9), we get

$$\sigma_{\dot{\vartheta}_1}^2 = \frac{\pi^2 f_m^2}{\eta_1^2 m_1 m_2}\left(\Omega_1 m_2 + \vartheta_1^2 s_1 m_1\right). \qquad (11)$$

Further, the joint PDF of ϑ_1, $\dot{\vartheta}_1$ and η_1 is

$$\begin{aligned} &p_{\vartheta_1\dot{\vartheta}_1\eta_1}(\vartheta_1,\dot{\vartheta}_1,\eta_1) \\ &= p_{\dot{\vartheta}_1}(\dot{\vartheta}_1 \mid \vartheta_1,\eta_1)\, p_{\vartheta_1\eta_1}(\vartheta_1,\eta_1) \qquad (12) \\ &= p_{\dot{\vartheta}_1}(\dot{\vartheta}_1 \mid \vartheta_1,\eta_1)\, p_{\eta_1}(\eta_1)\, p_{\vartheta_1}(\vartheta_1 \mid \eta_1), \end{aligned}$$

where

$$p_{\vartheta_1}(\vartheta_1 \mid \eta_1) = \left|\frac{\mathrm{d}\zeta_1}{\mathrm{d}\vartheta_1}\right| p_{\zeta_1}(\vartheta_1\eta_1), \quad \frac{\mathrm{d}\zeta_1}{\mathrm{d}\vartheta_1} = \eta_1.$$

Accordingly, the PDF is now

$$\begin{aligned} &p_{\vartheta_1\dot{\vartheta}_1\eta_1}(\vartheta_1,\dot{\vartheta}_1,\eta_1) \\ &= \eta_1 p_{\dot{\vartheta}_1}(\dot{\vartheta}_1 \mid \vartheta_1,\eta_1)p_{\eta_1}(\eta_1)p_{\zeta_1}(\vartheta_1\eta_1), \end{aligned} \qquad (13)$$

and the joint PDF of ϑ_1 and $\dot{\vartheta}_1$ is

$$\begin{aligned} &p_{\vartheta_1\dot{\vartheta}_1}(\vartheta_1,\dot{\vartheta}_1) \\ &= \int_0^{+\infty} \mathrm{d}\eta_1\, \eta_1 p_{\zeta_1}(\vartheta_1\eta_1)p_{\eta_1}(\eta_1)p_{\dot{\vartheta}_1}(\dot{\vartheta}_1 \mid \vartheta_1,\eta_1). \end{aligned} \qquad (14)$$

The LCR is obtained by averaging the joint PDF of a signal and its first derivative over the derivative, thus the LCR of ϑ_1 is (Panic *et al.*, 2013)

$$\begin{aligned} &N_{\vartheta_1}(\vartheta_1) \\ &= \int_0^{+\infty} \mathrm{d}\dot{\vartheta}_1\, \dot{\vartheta}_1 p_{\vartheta_1\dot{\vartheta}_1}(\vartheta_1,\dot{\vartheta}_1) \\ &= \int_0^{+\infty} \mathrm{d}\dot{\vartheta}_1\, \dot{\vartheta}_1 \int_0^{+\infty} \mathrm{d}\eta_1\, \eta_1 p_{\zeta_1}(\vartheta_1\eta_1)p_{\eta_1}(\eta_1)p_{\dot{\vartheta}_1}(\dot{\vartheta}_1 \mid \vartheta_1,\eta_1) \\ &= \int_0^{+\infty} \mathrm{d}\eta_1\, \eta_1 p_{\zeta_1}(\vartheta_1\eta_1)p_{\eta_1}(\eta_1) \int_0^{+\infty} \mathrm{d}\dot{\vartheta}_1\, \frac{\dot{\vartheta}_1 e^{-\frac{\dot{\vartheta}_1^2}{2\sigma_{\dot{\vartheta}_1}^2}}}{\sqrt{2\pi}\sigma_{\dot{\vartheta}_1}} \\ &= \frac{f_m}{2}\sqrt{\frac{\pi}{2}}\frac{\Gamma(m_1+m_2-1/2)}{\Gamma(m_1)\Gamma(m_2)} \\ &\quad \times \frac{(m_1 s_1)^{m_1-1/2}(m_2\Omega_1)^{m_2-1/2}}{(m_1 s_1\vartheta_1^2 + \Omega_1 m_2)^{m_1+m_2-1/2}}\vartheta_1^{2m_1-1}. \end{aligned} \qquad (15)$$

4. Outage statistics over the LOS signal path in the presence of interference

In this section we provide statistical measures such as (i) PDF, (ii) CDF and (iii) the LCR of the ratio of two Rice (R) RVs in order to address M2M communication over the LOS signal path in the presence of interference. Signal ζ_2 has the R PDF (Panic *et al.*, 2013)

$$\begin{aligned} p_{\zeta_2}(\zeta_2) &= 2\frac{\kappa_1+1}{\Omega_2 e^{\kappa_1}}\sum_{i_1=0}^{+\infty}\left(\kappa_1\frac{\kappa_1+1}{\Omega_2}\right)^{i_1} \\ &\quad \times \frac{\zeta_2^{2i_1+1}}{(i_1!)^2}\exp\left(-\frac{\kappa_1+1}{\Omega_2}\zeta_2^2\right), \quad \zeta_2 \geq 0. \end{aligned} \qquad (16)$$

Interference η_2 also has the Rician PDF (Panic *et al.*, 2013)

$$\begin{aligned} p_{\eta_2}(\eta_2) &= 2\frac{\kappa_2+1}{s_2 e^{\kappa_2}}\sum_{i_2=0}^{+\infty}\left(\kappa_2\frac{\kappa_2+1}{s_2}\right)^{i_2} \\ &\quad \times \frac{\eta_2^{2i_2+1}}{(i_2!)^2}\exp\left(-\frac{\kappa_2+1}{s_2}\eta_2^2\right), \quad \eta_2 \geq 0. \end{aligned} \qquad (17)$$

In an interference limited LOS environment, the ratio of ζ_2 and η_2 denoted by variable ϑ_2 can be expressed as (Milosevic *et al.*, 2018b; Talha and Patzold, 2011; Pavlović *et al.*, 2013; Stefanovic *et al.*, 2019; Wang *et al.*, 2008)

$$\vartheta_2 = \frac{\zeta_2}{\eta_2}. \tag{18}$$

The PDF of ϑ_2 is (Panic *et al.*, 2013)

$$\begin{aligned}
p_{\vartheta_2}(\vartheta_2) &= \int_0^{+\infty} d\eta_2 \, \eta_2 p_{\zeta_2}(\vartheta_2 \eta_2) p_{\eta_2}(\eta_2) \\
&= 2 \frac{(\kappa_1 + 1)(\kappa_2 + 1)}{\Omega_2 s_2 e^{\kappa_1 + \kappa_2}} \sum_{i_1=0}^{\infty} \left(\kappa_1 \frac{\kappa_1 + 1}{\Omega_2} \right)^{i_1} \\
&\quad \times \frac{\vartheta_2^{2i_1+1}}{(i_1!)^2} \sum_{i_2=0}^{+\infty} \frac{1}{(i_2!)^2} \left(\kappa_2 \frac{\kappa_2 + 1}{s_2} \right)^{i_2} \\
&\quad \times \frac{(\Omega_2 s_2)^{i_1+i_2+2} \Gamma(i_1 + i_2 + 2)}{((\kappa_1 + 1)s_2 \vartheta_2^2 + (\kappa_2 + 1)\Omega_2)^{i_1+i_2+2}}.
\end{aligned} \tag{19}$$

The CDF of ϑ_2 is (Panic *et al.*, 2013)

$$\begin{aligned}
& F_{\vartheta_2}(\vartheta_2) \\
&= \int_0^{\vartheta_2} dt \, p_{\vartheta_2}(t) \\
&= 2 \frac{(\kappa_1 + 1)(\kappa_2 + 1)}{e^{\kappa_1 + \kappa_2}} \Omega_2 s_2 \sum_{i_1=0}^{+\infty} \frac{\left(s_2 \kappa_1 (\kappa_1 + 1) \right)^{i_1}}{(i_1!)^2} \\
&\quad \times \sum_{i_2=0}^{+\infty} \frac{\left(\Omega_2 \kappa_2 (\kappa_2 + 1) \right)^{i_2}}{(i_2!)^2} \Gamma(i_1 + i_2 + 2) \\
&\quad \times \int_0^{\vartheta_2} \frac{t^{2i_1+1} \, dt}{((\kappa_1 + 1)s_2 t^2 + (\kappa_2 + 1)\Omega_2)^{i_1+i_2+2}}.
\end{aligned} \tag{20}$$

The previous integral can also be expressed in a simpler form by using the definition of the incomplete Beta function (Gradshteyn and Ryzhik, 2000). By the appropriate substitution we get

$$\begin{aligned}
& F_{\vartheta_2}(\vartheta_2) \\
&= \frac{1}{e^{\kappa_1 + \kappa_2}} \sum_{i_1=0}^{+\infty} \frac{\kappa_1^{i_1}}{(i_1!)^2} \sum_{i_2=0}^{+\infty} \frac{\kappa_2^{i_2}}{(i_2!)^2} \Gamma(i_1 + i_2 + 2) \\
&\quad \times B\left(\frac{(\kappa_1 + 1)s_2 \vartheta_2^2}{(\kappa_2 + 1)\Omega_2 + (\kappa_1 + 1)s_2 \vartheta_2^2}; \, i_1 + 1, i_2 + 1 \right).
\end{aligned} \tag{21}$$

It is easily proven that this series converges absolutely for arbitrary nonnegative ϑ_2, since $B(x; \, m, n) \le B(m, n)$ for $0 \le x \le 1$, and $m, n \ge 0$.

Therefore, $B(x; \, i_1 + 1, i_2 + 1) \le B(i_1 + 1, i_2 + 1) = i_1! i_2! / \Gamma(i_1 + i_2 + 2)$. Thus, the series is bounded above by $\left(\sum_{i_1=0}^{+\infty} \kappa_1^{i_1} / i_1! \right) \left(\sum_{i_2=0}^{+\infty} \kappa_2^{i_2} / i_2! \right)$, which is clearly $e^{\kappa_1 + \kappa_2}$. Since the terms in this series are nonnegative, the series is increasing while being bounded, and so it converges. Additionally, this last step proves that $0 \le F_{\vartheta_2}(\vartheta_2) \le 1$, as it should be by the probability normalization requirement.

We can make use of previous derivation to estimate the remainder when finite numbers of terms m, n are taken in the series. The error estimate for $F_{\vartheta_2}(\vartheta_2)$ is then

$$\begin{aligned}
R_{m,n} &\le \sum_{i_1=m}^{+\infty} \frac{\kappa_1^{i_1}}{i_1!} \sum_{i_2=n}^{+\infty} \frac{\kappa_2^{i_2}}{i_2!} \\
&= \left(1 - \frac{\Gamma(m, \kappa_1)}{(m-1)!} \right) \left(1 - \frac{\Gamma(n, \kappa_2)}{(n-1)!} \right),
\end{aligned} \tag{22}$$

where $\Gamma(i, x)$ represents the incomplete gamma function. The remainder drops sharply when m and n increase and it is usually sufficient to have $m, n \approx 10$ in order to obtain accurate results for small Rician factors κ_1, κ_2, while for large Rician factors (15 dB, for example), it may be required to have $m, n \approx 50$.

Next, random variable ϑ_2 and its time derivative are expressed as

$$\begin{aligned}
\vartheta_2 &= \frac{\zeta_2}{\eta_2}, \\
\dot{\vartheta}_2 &= \frac{\dot{\zeta}_2}{\eta_2} - \frac{\zeta_2}{\eta_2^2} \dot{\eta}_2,
\end{aligned} \tag{23}$$

where $\dot{\zeta}_2$, $\dot{\eta}_2$ and $\dot{\vartheta}_2$ are the first derivatives of ζ_2, η_2, and ϑ_2, respectively. Similarly, $\dot{\vartheta}_2$ has a Gaussian PDF (Jakes and Cox, 1994). The mean of $\dot{\vartheta}_2$ is

$$\overline{\dot{\vartheta}_2} = \frac{\overline{\dot{\zeta}_2}}{\eta_2} - \frac{\zeta_2}{\eta_2^2} \overline{\dot{\eta}_2} = 0,$$

since the mean values of $\dot{\zeta}_2$ and $\dot{\eta}_2$ are $\overline{\dot{\zeta}_2} = \overline{\dot{\eta}_2} = 0$. The variance of the ratio's fist derivative can be determined as

$$\sigma_{\dot{\vartheta}_2}^2 = \frac{1}{\eta_2^2} \sigma_{\dot{\zeta}_2}^2 + \frac{\zeta_2^2}{\eta_2^4} \sigma_{\dot{\eta}_2}^2, \tag{24}$$

where the variances of $\dot{\zeta}_2$ and $\dot{\eta}_2$ are

$$\sigma_{\dot{\zeta}_2}^2 = \pi^2 f_m^2 \frac{\Omega_2}{\kappa_1 + 1}, \quad \sigma_{\dot{\eta}_2}^2 = \pi^2 f_m^2 \frac{s_1}{\kappa_2 + 1}, \tag{25}$$

respectively.

Substituting (25) into (24), we get

$$\sigma_{\dot{\vartheta}_2}^2 = \frac{\pi^2 f_m^2 \left(\Omega_2(\kappa_2 + 1) + \vartheta_2^2 s_2(\kappa_1 + 1) \right)}{\eta_2^2 (\kappa_1 + 1)(\kappa_2 + 1)}. \tag{26}$$

The joint CDF of ϑ_2, $\dot{\vartheta}_2$ and η_2 is

$$p_{\vartheta_2 \dot{\vartheta}_2 \eta_2}(\vartheta_2, \dot{\vartheta}_2, \eta_2)$$
$$= p_{\dot{\vartheta}_2}(\dot{\vartheta}_2 \mid \vartheta_2, \eta_2) p_{\vartheta_2 \eta_2}(\vartheta_2, \eta_2) \qquad (27)$$
$$= p_{\dot{\vartheta}_2}(\dot{\vartheta}_2 \mid \vartheta_2, \eta_2) p_{\eta_2}(\eta_2) p_{\vartheta_2}(\vartheta_2 \mid \eta_2),$$

where

$$p_{\vartheta_2}(\vartheta_2 \mid \eta_2) = \left| \frac{\mathrm{d}\zeta_2}{\mathrm{d}\vartheta_2} \right| p_{\zeta_2}(\vartheta_2 \eta_2),$$

$$\frac{\mathrm{d}\zeta_2}{\mathrm{d}\vartheta_2} = \eta_2.$$

The CDF of ϑ_2, $\dot{\vartheta}_2$, and η_2, after substitution, is

$$p_{\vartheta_2 \dot{\vartheta}_2 \eta_2}(\vartheta_2, \dot{\vartheta}_2, \eta_2)$$
$$= p_{\dot{\vartheta}_2}(\dot{\vartheta}_2 \mid \vartheta_2, \eta_2) p_{\eta_2}(\eta_2) \eta_2 p_{\zeta_2}(\vartheta_2 \eta_2). \qquad (28)$$

Now, the joint CDF of ϑ_2 and $\dot{\vartheta}_2$ is

$$p_{\vartheta_2 \dot{\vartheta}_2}(\vartheta_2, \dot{\vartheta}_2)$$
$$= \int_0^{+\infty} \mathrm{d}\eta_2 \, \eta_2 p_{\zeta_2}(\vartheta_2 \eta_2) p_{\eta_2}(\eta_2) p_{\dot{\vartheta}_2}(\dot{\vartheta}_2 \mid \vartheta_2, \eta_2). \qquad (29)$$

We have already stated that the LCR is an important statistical variable of a random process. Accordingly, the LCR of ϑ_2 is (Panic *et al.*, 2013)

$$N_{\vartheta_2}(\vartheta_2)$$
$$= \int_0^{+\infty} \mathrm{d}\dot{\vartheta}_2 \, \dot{\vartheta}_2 p_{\vartheta_2 \dot{\vartheta}_2}(\vartheta_2, \dot{\vartheta}_2)$$
$$= \int_0^{+\infty} \mathrm{d}\eta_2 \, \eta_2 p_{\zeta_2}(\vartheta_2 \eta_2) p_{\eta_2}(\eta_2) \int_0^{+\infty} \mathrm{d}\dot{\vartheta}_2 \, \frac{\dot{\vartheta}_2 e^{-\frac{\dot{\vartheta}_2^2}{2\sigma_{\dot{\vartheta}_2}^2}}}{\sqrt{2\pi}\sigma_{\dot{\vartheta}_2}}$$
$$= f_m \frac{(2\pi\Omega_2 s_2 (\kappa_1 + 1)(\kappa_2 + 1))^{1/2}}{e^{\kappa_1 + \kappa_2}}$$
$$\times \sum_{i_1 = 0}^{+\infty} \frac{\kappa_1^{i_1} (\kappa_1 + 1)^{i_1} \vartheta_2^{2i_1 + 1}}{(i_1!)^2} \sum_{i_2 = 0}^{+\infty} \frac{\kappa_2^{i_2} (\kappa_2 + 1)^{i_2}}{(i_2!)^2}$$
$$\times \frac{\Gamma(i_1 + i_2 + 3/2)}{((\kappa_1 + 1)\vartheta_2^2 s_2 + (\kappa_2 + 1)\Omega_2)^{i_1 + i_2 + 1}}. \qquad (30)$$

5. Outage statistics at the output of the dual-branch AS reception system over the NLOS/LOS interference limited environment

This part provides statistical analysis in terms of the first- and second-order statistics such as (i) the PDF, (ii) the CDF and (iii) the LCR at the output of the dual-branch AS receiver of an MDN subjected to independent interference

limited NLOS and interference limited LOS channels at the first input and at the second input, respectively.

The conditional PDF of random variable ϑ, where $p_{\vartheta_1}(\vartheta_1 \mid s_1, \Omega_1)$, $F_{\vartheta_1}(\vartheta_1 \mid s_1, \Omega_1)$, $p_{\vartheta_2}(\vartheta_2 \mid s_2, \Omega_2)$ and $F_{\vartheta_2}(\vartheta_2 \mid s_2, \Omega_2)$ have already been determined in (4), (7), (19) and (21), respectively, is (Panic *et al.*, 2013)

$$p_\vartheta(\vartheta \mid s_1, s_2, \Omega_1, \Omega_2)$$
$$= p_{\vartheta_1}(\vartheta_1 \mid s_1, \Omega_1) F_{\vartheta_2}(\vartheta_2 \mid s_2, \Omega_2)$$
$$+ p_{\vartheta_2}(\vartheta_2 \mid s_2, \Omega_2) F_{\vartheta_1}(\vartheta_1 \mid s_1, \Omega_1)$$
$$= \frac{2}{\vartheta} \frac{\Gamma(m_1 + m_2)}{e^{\kappa_1 + \kappa_2} \Gamma(m_1)\Gamma(m_2)}$$
$$\times \sum_{i_1 = 0}^{+\infty} \sum_{i_2 = 0}^{+\infty} \frac{\kappa_1^{i_1}}{(i_1!)^2} \frac{\kappa_2^{i_2}}{(i_2!)^2} \Gamma(i_1 + i_2 + 2)$$
$$\times \left[\frac{(m_1 s_1 \vartheta^2)^{m_1} (m_2 \Omega_1)^{m_2}}{(m_1 s_1 \vartheta^2 + m_2 \Omega_1)^{m_1 + m_2}} \right.$$
$$\times \mathrm{B}\left(\frac{(\kappa_1 + 1)s_2 \vartheta^2}{(\kappa_2 + 1)\Omega_2 + (\kappa_1 + 1)s_2 \vartheta^2}; \ i_1 + 1, i_2 + 1 \right)$$
$$+ \mathrm{B}\left(\frac{m_1 s_1 \vartheta^2}{m_2 \Omega_1 + m_1 s_1 \vartheta^2}; \ m_1, m_2 \right)$$
$$\left. \times \frac{\left((\kappa_1 + 1)s_1 \vartheta^2\right)^{i_1} \left((\kappa_2 + 1)\Omega_1\right)^{i_2}}{\left((\kappa_1 + 1)s_2 \vartheta^2 + (\kappa_2 + 1)\Omega_2\right)^{i_1 + i_2 + 2}} \right], \qquad (31)$$

where $\mathrm{B}(x; a, b)$ signifies the incomplete Beta function (Gradshteyn and Ryzhik, 2000). In much the same way as in the proof that (21) converges, it is straightforward to prove that the previous equation also converges fast.

It has been already stated by Panic *et al.* (2013), Kostić (2005), Shankar (2004) or Jakes and Cox (1994) that the shadowing effect is characterized by variation in signal powers. The probability density at the output of an dual-branch AS receiver of the MDN depends on s_1, s_2, Ω_1 and Ω_2. Parameter s_1 represents the interference power at the first input and s_2 is the interference power at the second input of the AS receiver while parameter Ω_1 is the power of the desired signal at the first input and parameter Ω_2 is the signal power at the second input of the AS receiver. In order to account for the impact of shadowing as in the works of Panic *et al.* (2013), Kostić (2005), Shankar (2004) or Jakes and Cox (1994), we suppose that the PDFs of s_1, s_2, Ω_1 and Ω_2 are Gamma PDFs, respectively,

$$p_{s_{1/2}}(x) = \frac{1}{\Gamma(c_1)\beta_{1/2}^{c_1}} x^{c_1 - 1} e^{-\frac{1}{\beta_{1/2}}x}, \qquad x \geq 0, \quad (32)$$

$$p_{\Omega_{1/2}}(x) = \frac{1}{\Gamma(c_2)\alpha_{1/2}^{c_2}} x^{c_2 - 1} e^{-\frac{1}{\alpha_{1/2}}x}, \qquad x \geq 0, \quad (33)$$

where c_1 and c_2 are shape parameters (related to the severity of shadowing) of the interference and the desired signal, respectively, while scale parameters are β_i and

α_i, regarding the interferences and the desired signals, respectively.

Following the results reported by Panic *et al.* (2013), we obtain the conditional CDF of ϑ, where $F_{\vartheta_1}(\vartheta_1 \mid s_1, \Omega_1)$ and $F_{\vartheta_2}(\vartheta_2 \mid s_2, \Omega_2)$ have already been obtained in (7) and (21), respectively

$$
F_\vartheta(\vartheta \mid s_1, s_2, \Omega_1, \Omega_2) \tag{34}
$$
$$
= F_{\vartheta_1}(\vartheta_1 \mid s_1, \Omega_1) F_{\vartheta_2}(\vartheta_2 \mid s_2, \Omega_2)
$$
$$
= \frac{1}{e^{\kappa_1 + \kappa_2}} \frac{\Gamma(m_1 + m_2)}{\Gamma(m_1)\Gamma(m_2)}
$$
$$
\times \mathrm{B}\left(\frac{m_1 s_1 \vartheta^2}{m_2 \Omega_1 + m_1 s_1 \vartheta^2}; \ m_1, m_2 \right)
$$
$$
\times \sum_{i_1=0}^{+\infty} \frac{\kappa_1^{i_1}}{(i_1!)^2} \sum_{i_2=0}^{+\infty} \frac{\kappa_2^{i_2}}{(i_2!)^2} \Gamma(i_1 + i_2 + 2)
$$
$$
\times \mathrm{B}\left(\frac{(\kappa_1 + 1)s_2 \vartheta^2}{(\kappa_2 + 1)\Omega_2 + (\kappa_1 + 1)s_2 \vartheta^2}; \ i_1 + 1, i_2 + 1 \right).
$$

Finally, the PDF and the CDF of ϑ at the output of the dual-branch AS receiver of MDN for the proposed M2M communications over interference limited dissimilar composite fading channels are

$$
p_\vartheta(\vartheta) = \int_0^{+\infty} \mathrm{d}s_1 \, p_{s_1}(s_1) \int_0^{+\infty} \mathrm{d}s_2 \, p_{s_2}(s_2) \int_0^{+\infty} \mathrm{d}\Omega_1 \, p_{\Omega_1}(\Omega_1)
$$
$$
\int_0^{+\infty} \mathrm{d}\Omega_2 \, p_{\Omega_2}(\Omega_2) p_\vartheta(\vartheta \mid s_1, s_2, \Omega_1, \Omega_2). \tag{35}
$$

$$
F_\vartheta(\vartheta)
$$
$$
= \int_0^{+\infty} \mathrm{d}s_1 \, p_{s_1}(s_1) \int_0^{+\infty} \mathrm{d}s_2 \, p_{s_2}(s_2) \int_0^{+\infty} \mathrm{d}\Omega_1 \, p_{\Omega_1}(\Omega_1)
$$
$$
\int_0^{+\infty} \mathrm{d}\Omega_2 \, p_{\Omega_2}(\Omega_2) F_\vartheta(\vartheta \mid s_1, s_2, \Omega_1, \Omega_2). \tag{36}
$$

The conditional joint CDF of ϑ and $\dot\vartheta$ is

$$
p_{\vartheta, \dot\vartheta}(\vartheta, \dot\vartheta \mid s_1, s_2, \Omega_1, \Omega_2)
$$
$$
= p_{\vartheta_1, \dot\vartheta_1}(\vartheta, \dot\vartheta \mid s_1, \Omega_1) \tag{37}
$$
$$
\times F_{\vartheta_2}(\vartheta_1 \mid s_2, \Omega_2)
$$
$$
+ p_{\vartheta_2, \dot\vartheta_2}(\vartheta, \dot\vartheta \mid s_2, \Omega_2) F_{\vartheta_1}(\vartheta_1 \mid s_1, \Omega_1).
$$

The LCR can be determined by averaging the conditional number of crossing rates. Some of the LCR parameters, such as Doppler frequency, signal powers, m parameters or κ parameters, may vary. The Doppler frequency also depends on several parameters that can be independent. Therefore, it can be assumed that the Doppler frequency

has a Gaussian PDF as the consequence of the Central Limit Theorem (Jakes and Cox, 1994). This is important since the variance depends on the Doppler frequency and the conditional LCR of ϑ, where N_{ϑ_1}, $F_{\vartheta_1}(\vartheta_1 \mid s_1, \Omega_1)$, N_{ϑ_2} and $F_{\vartheta_2}(\vartheta_2 \mid s_2, \Omega_2)$ have already been obtained in (15), (7), (30) and (21), respectively.

We have

$$
N_{\vartheta \mid s_1, s_2, \Omega_1, \Omega_2}
$$
$$
= \int_0^{+\infty} \mathrm{d}\dot\vartheta \, \dot\vartheta \, p_{\vartheta, \dot\vartheta}(\vartheta, \dot\vartheta \mid s_1, s_2, \Omega_1, \Omega_2)
$$
$$
= f_m \frac{\sqrt{\pi}}{e^{\kappa_1 + \kappa_2} \Gamma(m_1)\Gamma(m_2)} \left\{ (2\Omega_2 s_2(\kappa_1 + 1)(\kappa_2 + 1))^{1/2} \right.
$$
$$
\times \Gamma(m_1 + m_2) \mathrm{B}\left(\frac{m_1 s_1 \vartheta^2}{m_2 \Omega_1 + m_1 s_1 \vartheta^2}; \ m_1, m_2 \right)
$$
$$
\times \sum_{i_1=0}^{+\infty} \frac{(\kappa_1 s_2(\kappa_1 + 1))^{i_1}}{(i_1!)^2} \vartheta^{2i_1 - 1} \sum_{i_2=0}^{\infty} \frac{(\kappa_2 \Omega_2(\kappa_2 + 1))^{i_2}}{(i_2!)^2}
$$
$$
\times \frac{\Gamma(i_1 + i_2 + 3/2)}{((\kappa_2 + 1)\Omega_2 + (\kappa_1 + 1)s_2 \vartheta^2)^{i_1 + i_2 + 1}} \tag{38}
$$
$$
+ \left(\frac{1}{8 m_1 m_2 \Omega_1 s_1} \right)^{1/2} \frac{m_1^{m_1} m_2^{m_2} \vartheta^{2m_1 - 1}}{(m_2 \Omega_1 + m_1 s_1 \vartheta^2)^{m_1 + m_2 - 1}}
$$
$$
\times \sum_{i_1=0}^{+\infty} \frac{\kappa_1^{i_1}}{(i_1!)^2} \sum_{i_2=0}^{+\infty} \frac{\kappa_2^{i_2}}{(i_2!)^2} \Gamma(i_1 + i_2 + 2)
$$
$$
\left. \times \mathrm{B}\left(\frac{(\kappa_1 + 1)s_2 \vartheta^2}{(\kappa_2 + 1)\Omega_2 + (\kappa_1 + 1)s_2 \vartheta^2}; \ i_1 + 1, i_2 + 1 \right) \right\}.
$$

The LCR depends on the average signal power that varies slowly over time. The average interference power behaves in the same way. Based on that, the LCR at the output of the dual-branch AS receiver of the MDN over interference limited LOS/NLOS composite channels can be determined by averaging,

$$
N_\vartheta = \int_0^{+\infty} \mathrm{d}s_1 \, p_{s_1}(s_1) \int_0^{+\infty} \mathrm{d}s_2 \, p_{s_2}(s_2) \int_0^{+\infty} \mathrm{d}\Omega_1 \, p_{\Omega_1}(\Omega_1)
$$
$$
\int_0^{+\infty} \mathrm{d}\Omega_2 \, p_{\Omega_2}(\Omega_2) N_{\vartheta \mid s_1, s_2, \Omega_1, \Omega_2}. \tag{39}
$$

In order to certify the quality of service of the proposed model, we have analyzed the channel capacity further. The channel capacity, denoted by c, is defined as a maximum rate at which information can be transmitted through a channel of a specified bandwidth, denoted by B (Panic *et al.*, 2013; Jakes and Cox, 1994). To this end, we have used the well-known Shannon–Hartley theorem
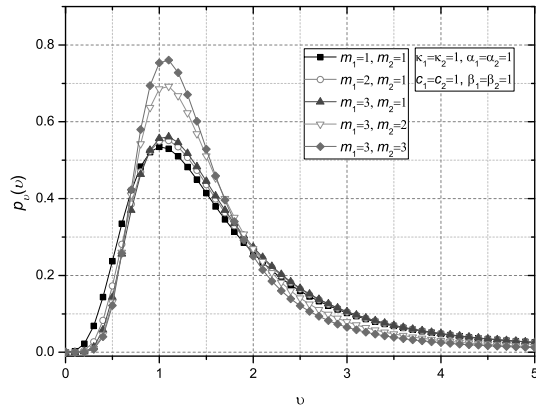
Fig. 3. PDF at the output of a two-input AS receiver for different values of the fading sharpness parameters m_1 and m_2.

Fig. 4. PDF at the output of a two-input AS receiver for different values of the Rice factors κ_1 and κ_2.

(Panic *et al.*, 2013) as follows:

$$\frac{c}{B} = \int_0^{+\infty} d\vartheta \, \log\left(1 + \vartheta^2\right) p_\vartheta(\vartheta) \tag{40}$$

$$= \int_0^{+\infty} d\vartheta \, \log\left(1 + \vartheta^2\right) \int_0^{+\infty} ds_1 \, p_{s_1}(s_1) \int_0^{+\infty} ds_2 \, p_{s_2}(s_2)$$

$$\int_0^{+\infty} d\Omega_1 \, p_{\Omega_1}(\Omega_1)$$

$$\int_0^{+\infty} d\Omega_2 \, p_{\Omega_2}(\Omega_2) p_\vartheta(\vartheta \mid s_1, s_2, \Omega_1, \Omega_2).$$

6. Numerical results

In this section, several numerically evaluated performance results are provided. These results include the PDF at the output of a two-input AS receiver for different values of sharpness parameters, the PDF at the output of a two-input AS receiver for different values of the Rice parameters, as well as the CDFs at the output of a two-input AS receiver for different values of the above-mentioned parameters. Also, in order to better present the obtained results, we provided a graphical representation of the CDF of the SIR, normalized signal LCR at the output of the two-input the SC receiver and the channel capacity at the output of a two-input AS receiver.

First, the expression (35) is graphically represented in Fig. 3 which gives us the PDF of the SIR at the output of the two-input AS receiver at the MDN. It is presented with the equal parameters $\kappa_1 = \kappa_2 = 1$, $\alpha_1 = \alpha_2 = 1$, $c_1 = c_2 = 1$, $\beta_1 = \beta_2 = 1$, and for different values of the multipath fading severity parameters m_1 and m_2. An increase in the value of the fading severity parameters m_1 and m_2 results in a narrowing of the range of the
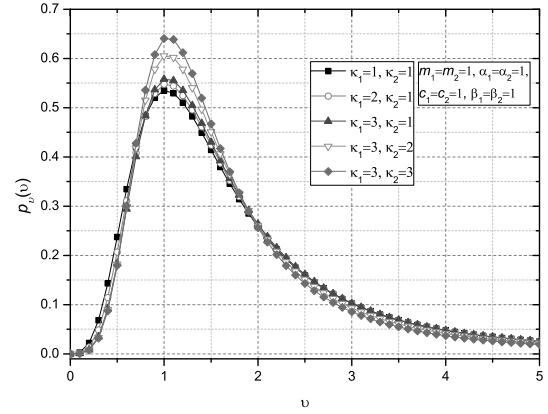
signal's PDF at the reception, as well as an increase in the maximum value reached for higher values of the received SIR.

In Fig. 4, the PDF of the SIR at the output of the two-input AS receiver at the MDN is plotted. It is presented with the equal parameters m_1, m_2, α_1, α_2, c_1, c_2, β_1 and β_2, and for different values of the Rice parameters κ_1 and κ_2. An increase in the values of the Rice parameters κ_1 and κ_2 results in a narrowing of the range of the signal's PDF at the reception, as well as an increase in the maximum value that is reached by higher values of the Rice parameters, but the increase in the PDF is more emphasized as the parameters m_1 and m_2 increase.

Figure 5 shows the CDF of the SIR at the output of the receiver with two inputs, for different system model parameters. Based on the analytical expression and the numerical results obtained, it can be concluded that with as ϑ increases, the CDF tends to one. Moreover, for higher values of the Rice factor κ_1 (κ_1 is related to the LOS desired signal component), a decrease in the Rice factor κ_2 (κ_2 is related to the LOS interference signal component) leads to a decrease in the CDF, which in turn yields a system performance improvement, as expected. A similar trend can be noticed for fading severity parameters of the desired signal and interference signal, m_1 and m_2. The decrease in the CDF is more emphasized for higher values of the Rice factor κ_1 and lower values of κ_2 than for higher values of fading severity parameters m_1 and lower values of m_2.

In order to explore the impact of the fading severity parameter of the desired signal on the CDF at the output of a two-input AS receiver, we present the CDF of the SIR versus the severity parameter m_1 in Fig. 6. The parameters α_1, α_2, c_1, c_2, β_1 and β_2 are equal while the values of the Rice factor parameters κ_1 and κ_2 and the severity parameters m_1 and m_2 are different. It can be noticed that the system performance improvement
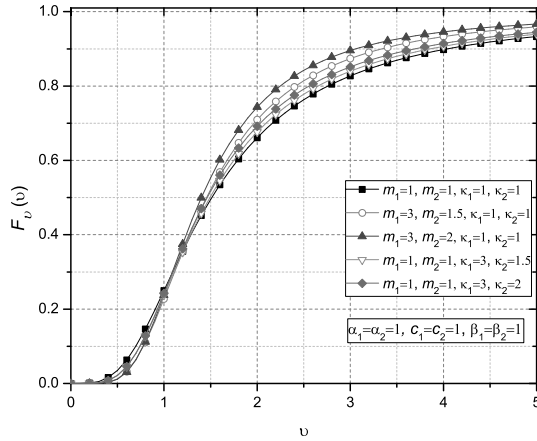
Fig. 5. CDF of SIR at the output of a two-input AS receiver for different values of the fading severity parameters m_1 and m_2, and with different values of Rice's κ_1 and κ_2 factors.
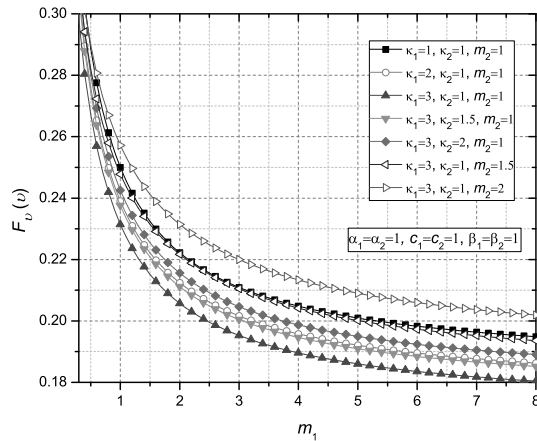

Fig. 6. CDF at the output of the two-input AS receiver vs. m_1, for different values of the fading severity parameter m_2 and different values of the Rice factors κ_1 and κ_2.

Fig. 7. CDF at the output of the two-input AS receiver vs. the Rice factor κ_1, for different values of fading severity parameters m_1 i m_2 and different values of the Rice factor κ_2.

Fig. 8. Normalized signal LCR at the output of the two-input SC receiver, for different values of fading severity parameters m_1 and m_2, and different values of the Rice factors κ_1 and κ_2.

is achieved by an increase in m_1 for all system model parameters considered, since the CDF decreases. The significant improvement in terms of the CDF for examined curves is achieved for higher values of κ_1 and lower values of κ_2 and m_2 (for example when $\kappa_1 = 3$, $\kappa_2 = 1$ and $m_2 = 1$). Figure 7 shows the CDF signal at the output of a two-input SC receiver versus the Rice factor κ_1. Similarly as in Fig. 6, only the Rice factor parameters κ_1 and κ_2 and the severity parameters m_1 and m_2 vary. It is obvious that the system performance improvement is achieved by an increase in κ_1 for all curves considered, since the CDF decreases. Moreover, a further performance improvement in terms of the CDF for the examined curves is achieved for higher values of m_1 and lower values of κ_2 and m_2 (for example, when $m_1 = 3$, $\kappa_2 = 1$ and $m_2 = 1$).

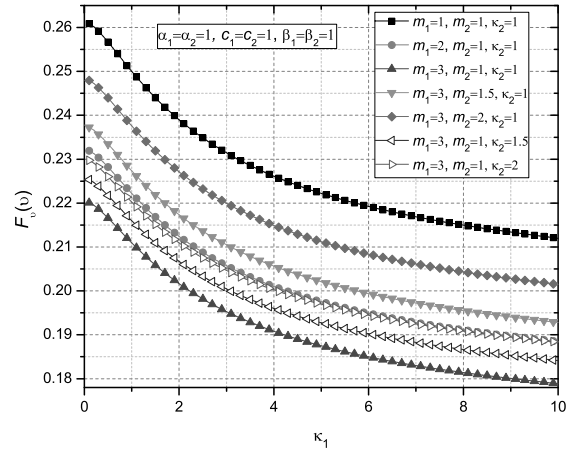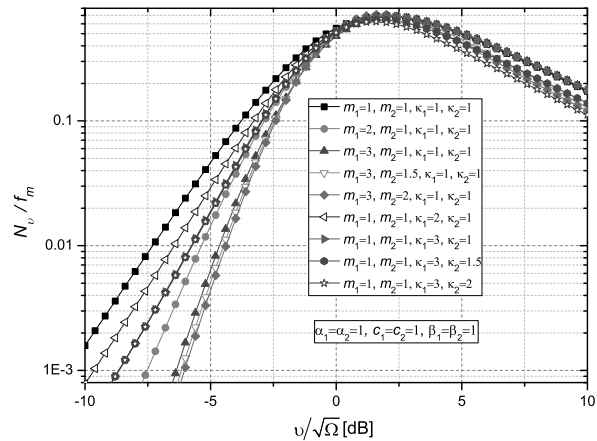Figure 8 is obtained based on (39) and it presents the LCR of the SIR at the output of the two-input AS receiver of the MDN. It shows the normalized LCR versus ϑ normalized by the square root of the mean value of the signal power Ω. The figure is presented for $\Omega = \Omega_1 = \Omega_2$, constant values of parameters α_1, α_2, c_1, c_2, β_1, and β_2, and different values of Rice factors κ_1, κ_2, and severity parameters m_1, m_2. It is noticeable that an increase in Rice's factor and a severity fading parameter of the desired signal yields a decrease in the LCR, especially in a lower dB output regime, which in turn enables more stable system performances.

Based on (40) we can graphically present the channel capacity at the output of the two-inputs AS receiver.

Figure 9 shows the channel capacity at the output of the two-input SC receiver, depending on the fading sharpness parameter m_1. Based on the analytical and numerical results obtained, the channel capacity for different values of the parameters m_2, κ_1, κ_2 and constant
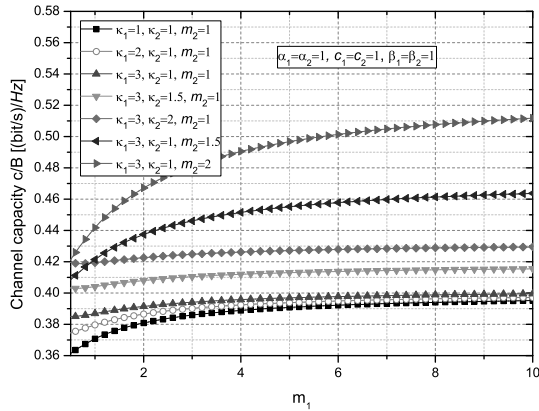
Fig. 9. Channel capacity at the output of the two-input AS receiver, depending on the fading sharpness parameter m_1.
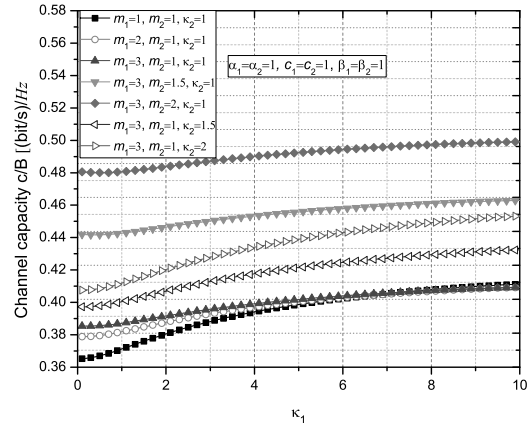

Fig. 11. Channel capacity at the output of the two-input SC receiver, depending on the Rice factor κ_1.
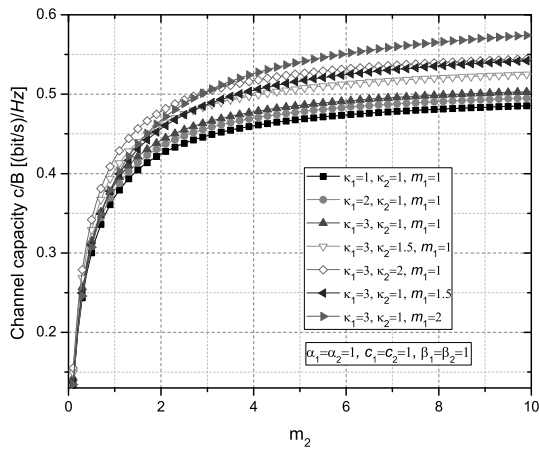

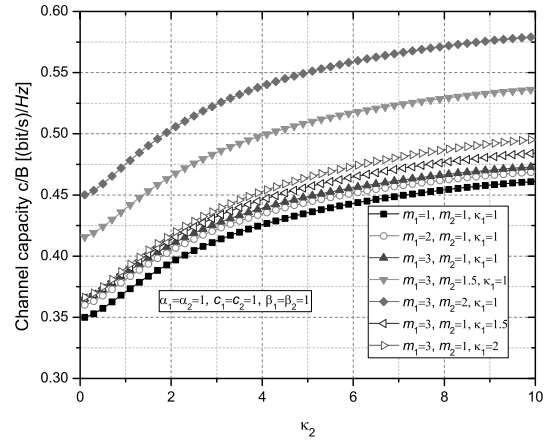Fig. 10. Channel capacity at the output of the two-input SC receiver, depending on the fading shaping parameter m_2.

Fig. 12. Channel capacity at the output of the two-input SC receiver, depending on the Rice factor κ_2.

values of the parameters α_1, α_2, c_1, c_2, β_1, and β_2, are graphically presented. Increasing the values of parameters m_2, κ_1 and κ_2 results in an increase in the channel capacity.

Based on (40) we can graphically present the channel capacity at the output of the two-input AS receiver. Figure 10 shows the channel capacity at the output of the two-input SC receiver, depending on the fading sharpness parameter m_2. Based on the obtained analytical and numerical results, the channel capacity for various values of parameters m_1, κ_1 and κ_2 and constant values of parameters α_1, α_2, c_1, c_2, β_1, and β_2 are graphically presented. Increasing the values of parameters m_1, κ_1 and κ_2 results in an increase in channel capacity.

Figure 11 shows channel capacity at the output of two-input SC receiver, depending on the Rice factor κ_1. Based on the analytical and numerical results obtained, the channel capacity for various values of parameters m_1, m_2, κ_2 and constant values of α_1, α_2, c_1, c_2, β_1,

and β_2 are graphically presented. Increasing the values of parameters m_1, m_1 and κ_2 results in an increase in channel capacity.

Figure 12 shows channel capacity at the output of the two-input SC receiver, depending on the Rice factor κ_2. Based on the obtained analytical and numerical results, the channel capacity for various values of the parameters m_1, m_2, κ_1 and constant values of the parameters α_1, α_2, c_1, c_2, β_1, and β_2 are graphically presented. Increasing the values of parameters m_1, m_1 and κ_1 results in an increase in channel capacity. Previous figures show that by an increase of the parameters m_1 and κ_2, the highest channel capacity is obtained.

7. Conclusion

Direct mobile-to-mobile communications with a two-input antenna selection (AS) system at a destination mobile node have been considered in interference limited,

LOS/NLOS composite fading environments, modeled as (i) the ratio of two Nakagami-m (N) random variables (RVs) at the first input and (ii) as the ratio of two Rice RVs at the second input of AS receiver. We have obtained the first- and second-order statistics in closed form such as the probability density function, the cumulative distribution function and the average level crossing rate at the output of the AS receiver of the MDN. Capitalizing on this results, we have taken into account an AS based algorithm of mean power variation at the system's output and derived and graphically presented results for all statistical measures considered.

The obtained results show that the system performance can be significantly improved by ameliorated values of the LOS factor and the fading severity parameter of the desired signal while interference stays with a low LOS factor and has more severe fading. Practically, this means that the transmitter and the receiver have good optical views of each other, and that interference is not generated by the same transmitter or the transmitters that are positioned in the same direction. When there is no permanent LOS communication, the desired signal is NLOS, which results in poor performance and lower channel capacity. Small values of the fading parameter correspond to a channel that experiences strong fading, while an increasing parameter value indicates that the environment is gradually transitioning from NLOS towards LOS conditions. Moreover, it is also evident that higher values of the corresponding fading parameter and resulting less severe fading can still provide satisfactory system performances. In our future work, we will demonstrate some experimental results to verify these theoretical findings.

Acknowledgment

References

Abdi, A., Gao, C. and Haimovich, A.M. (2003). Level crossing rate and average fade duration in MIMO mobile fading channels, *2003 IEEE 58th Vehicular Technology Conference, Orlando, USA*, pp. 3164–3168.

Agiwal, M., Roy, A. and Saxena, N. (2016). Next generation 5G wireless networks: A comprehensive survey, *IEEE Communications Surveys and Tutorials* **18**(3): 1617–1655.

Bithas, P., Efthymoglou, G. and Kanatas, A. (2018a). V2V cooperative relaying communications under interference and outdated CSI, *IEEE Transactions on Vehicular Technology* **67**(4): 3466–3480.

Bithas, P., Kanatas, A., da Costa, D. and Upadhyay, P. (2018b). A low complexity communication technique for mobile-to-mobile communication systems, *14th IEEE International Wireless Communications & Mobile Computing Conference (IWCMC), Limassol, Cyprus*, pp. 400–405.

Bithas, P., Kanatas, A., da Costa, D., Upadhyay, P. and Dias, U. (2017). On the double-generalized gamma statistics and their application to the performance analysis of V2V communications, *IEEE Wireless Communications* **66**(1): 448–460.

Bithas, P.S., Nikolaidis, V., Kanatas, A.G. and Karagiannidis, G.K. (2020). UAV-to-ground communications: Channel modeling and UAV selection, *IEEE Transactions on Communications* **68**(8): 5135–5144.

Dixit, D., Kumar, N., Sharma, S., Bhatia, V., Panic, S. and Stefanovic, C. (2021). On the ASER performance of UAV-based communication systems for QAM schemes, *IEEE Communications Letters* **25**(6): 1835–1838.

Djosic, D., Stefanovic, C., Milic, D. and Stefanovic, M. (2019). System performances of SC reception in asymmetric multipath fading environments, *The University Thought, Publication in Natural Sciences* **9**(2): 56–62.

Djošić, D., Milošević, N., Nikolić, Z., Dimitrijević, B., Bandjur, M. and Stefanović, M. (2017). Statistics of signal to interference ratio process at output of mobile-to-mobile Rayleigh fading channel in the presence of cochannel interference, *Facta Universitatis, Automatic Control and Robotics* **16**(2): 185–196.

Gradshteyn, I.S. and Ryzhik, I.M. (2000). *Table of Integrals, Series, and Products, 6th Edn*, Academic Press, New York.

Hajri, N., Khedhiri, R. and Youssef, N. (2020). On selection combining diversity in dual-hop relaying systems over double Rice channels: Fade statistics and performance analysis, *IEEE Access* **8**: 72188–72203, DOI: 10.1109/ACCESS.2020.2986142.

Huang, C., Wang, R., Tang, P., He, R., Ai, B., Zhong, Z., Oestges, C. and Molisch, A. F. (2020). Geometry-cluster-based stochastic MIMO model for vehicle-to-vehicle communications in street canyon scenarios, *IEEE Transactions on Wireless Communications* **20**(2): 755–770.

Ivanis, P., Drajic, D. and Vucetic, B. (2007). Level crossing rates of Ricean MIMO channel eigenvalues for imperfect and outdated CSI, *IEEE Communications Letters* **11**(10): 775–777.

Jaiswal, N. and Purohit, N. (2021). Performance analysis of NOMA-enabled vehicular communication systems with transmit antenna selection over double Nakagami-m fading, *IEEE Transactions on Vehicular Technology* **70**(12): 12725–12741.

Jakes, W.C. and Cox, D.C. (1994). *Microwave Mobile Communications*, Wiley/IEEE Press, Hoboken.

Khedhiri, R., Hajri, N., Youssef, N. and Pätzold, M. (2014). On the first-and second-order statistics of selective combining over double Nakagami-m fading channels, *Proceedings*

of the 80th IEEE Vehicular Technology Conference (VTC2014–Fall), Vancouver, Canada, pp. 1–5.

Kostić, I. (2005). Analytical approach to performance analysis for channel subject to shadowing and fading, *IEE Proceedings—Communications* **152**(6): 821–827.

Marins, T.R.R., Dos Anjos, A.A., Da Silva, C.R.N., Peñarrocha, V.M.R., Rubio, L., Reig, J., De Souza, R.A.A. and Yacoub, M.D. (2021). Fading evaluation in standardized 5G millimeter-wave band, *IEEE Access* **9**: 67268–67280, DOI: 10.1109/ACCESS.2021.3076631.

Milenkovic, V., Panic, S., Denic, D. and Radenkovic, D. (2017). Novel method for 5G systems NLOS channels parameter estimation, *International Journal of Antennas and Propagation* **2017**, Article ID: 5236246, DOI: 10.1155/2017/5236246.

Milic, D., Djosic, D., Stefanovic, C., Panic, S. and Stefanovic, M. (2016). Second order statistics of the SC receiver over Rician fading channels in the presence of multiple Nakagami-m interferers, *International Journal of Numerical Modelling: Electronic Networks, Devices and Fields* **29**: 222–229, DOI: 10.1002/jnm.2065.

Milosevic, N., Stefanovic, C., Nikolic, Z., Bandjur, M. and Stefanovic, M. (2018a). First- and second-order statistics of interference-limited mobile-to-mobile Weibull fading channel, *Journal of Circuits, Systems and Computers* **27**(11): 1850168.

Milosevic, N., Stefanovic, M., Nikolic, Z., Spalevic, P. and Stefanovic, C. (2018b). Performance analysis of interference-limited mobile-to-mobile $\kappa - \mu$ fading channel, *Wireless Personal Communications* **101**(3): 1685–1701.

Mumtaz, S., Huq, K. and Rodriguez, J. (2014). Direct mobile-to-mobile communication: Paradigm for 5G, *IEEE Wireless Communications* **21**(5): 14–23.

Panic, S., Stefanovic, M., Anastasov, J. and Spalevic, P. (2013). *Fading and Interference Mitigation in Wireless Communications*, CRC Press, New York.

Pavlović, D.H., Sekulović, N.M., Milovanović, G.V., Panajotović, A.S., Stefanović, Č.M. and Popović, J. Z. (2013). Statistics for ratios of Rayleigh, Rician, Nakagami–m, and Weibull distributed random variables, *Mathematical Problems in Engineering* **2013**, Article no. 252804.

Sekulović, N., Panajotović, A., Drača, D., Stefanović, M. and Bandjur, M. (2018). Investigation into diversity order at micro and/or macro level in gamma shadowed Nakagami-m fading channels, *International Journal of Numerical Modelling: Electronic Networks, Devices and Fields* **31**: e2288, DOI: 10.1002/jnm.2288.

Shankar, P. (2004). Error rates in generalized shadowed fading channels, *Wireless Personal Communications* **28**: 233–238, DOI: 10.1023/B:wire.0000032253.68423.86.

Silva, C.D., Bhargav, N., Leonardo, E. and Yacoub, M. (2019). Ratio of two envelopes taken from $\alpha - \mu$, $\kappa - \mu$, and $\eta - \mu$ variates and some practical applications, *IEEE Access* **214**(2): 256–261.

Stefanovic, C., Panic, S., Bhatia, V. and Kumar, N. (2021). On second-order statistics of the composite channel models for UAV-to-ground communications with UAV selection, *IEEE Open Journal of the Communications Society* **2**: 534–544, DOI: 10.1109/OJCOMS.2021.3064873.

Stefanovic, C., Pratesi, M. and Santucci, F. (2018a). Performance evaluation of cooperative communications over fading channels in vehicular networks, *2018 2nd URSI Atlantic Radio Science Meeting (AT-RASC), Meloneras, Spain*, pp. 1–4.

Stefanovic, C., Veljkovic, S., Stefanovic, M., Panic, S. and Jovkovic, S. (2018b). Second order statistics of SIR based macro diversity system for V2I communications over composite fading channels, *First International Conference on Secure Cyber Computing and Communication (ICSCCC), Jalandhar, India*, pp. 569–573.

Stefanovic, D., Stefanovic, C., Djosic, D., Milic, D., Rancic, D. and Stefanovic, M. (2019). LCR of the ratio of the product of two squared Nakagami-m random processes and its application to wireless communication systems, *2019 18th International Symposium (INFOTEH), Jahorina, Bosnia and Herzegovina*, pp. 1–4.

Sun, W., Shen, L., Shao, H. and Liu, P. (2021). Dynamic location models of mobile sensors for travel time estimation on a freeway, *International Journal of Applied Mathematics and Computer Science* **31**(2): 271–287, DOI: 10.34768/amcs-2021-0019.

Talha, B. and Patzold, M. (2011). Channel models for mobile-to-mobile cooperative communication systems: A state of the art review, *IEEE Vehicular Technology Magazine* **6**(2): 33–43.

Wang, L.C., Liu, W.C. and Cheng, Y.H. (2008). Statistical analysis of a mobile-to-mobile Rician fading channel model, *IEEE Transactions on Vehicular Technology* **58**(1): 32–38.

Wu, J. and Fan, P. (2016). A survey on high mobility wireless communications: Challenges, opportunities and solutions, *IEEE Access* **4**: 450–476, DOI: 10.1109/ACCESS.2016.2518085.

Danijel B. Đošić was born in Priština, Serbia, in 1983. He obtained his MSc in computer science at the Faculty of Mathematics and Natural Sciences, University of Priština, in 2008. He received his PhD in the area of telecommunications at the Electronic Faculty of the University of Niš in 2019. His major research interests include wireless mobile and computer networks software applications. Currently, he works as an assistant professor at the Department of Informatics, Faculty of Natural Science and Mathematics, University of Priština.

Dejan Milić received his Dipl-Ing, MSc, and PhD degrees in electrical engineering from the Faculty of Electronic Engineering, University of Niš, Serbia, in 1997, 2001 and 2005, respectively. He currently holds a full professorial position at the Department of Telecommunications there, teaching optical communications and coherent communication systems. Other areas of his research include communication theory, modulation and wireless systems.

Srđan Milosavljević was born in Kosovska Mitrovica, Serbia, in 1980. He received his PhD degree from the Faculty of Electronics, University of Niš, Serbia. His primary research interests are information and communication technologies. He currently works as an assistant professor at the Faculty of Economics, University of Priština in Kosovska Mitrovica.

Nataša Kontrec was born in Kosovska Mitrovica in 1978. She received her PhD in mathematics in 2015 from the University of Priština in Kosovska Mitrovica, Faculty of Sciences and Mathematics. She is currently an associate professor of the Department of Mathematics at the same faculty. Her main research fields are predictive modeling and optimization.

Dušan M. Stefanović received his MSc and PhD degrees in telecommunications from the Faculty of Electronic Engineering, University of Niš, Serbia, in 2005 and 2012, respectively. He is currently a professor at the College of Applied Technical Sciences in Niš. His major research interests include wireless and optical communications, as well as mobile and computer networks. He also holds CISCO and Microsoft certifications such as CCNP and MCSE.

Časlav Stefanović was born in Niš, Serbia in 1982. He received MSc and PhD degrees in electrical engineering from the Faculty of Electronic Engineering, University of Niš, in 2007, and 2017, respectively. Before joining he Department of Signal Theory and Communications at the Charles III University of Madrid in 2021, he was with the Department of Informatics, University of Priština in Kosovska Mitrovica, Serbia. His research interests are in the field of mobile and multi-channel communications, including statistical characterization and modeling of fading channels.